

Er₂Ti₂O₇: Evidence of quantum order by disorder in a frustrated antiferromagnet

J. D. M. Champion,^{1,2,3} M. J. Harris,² P. C. W. Holdsworth,³ A. S. Wills,⁴ G. Balakrishnan,⁵ S. T. Bramwell,^{1,*} E. Čížmár,⁶ T. Fennell,⁷ J. S. Gardner,^{8,9} J. Lago,¹ D. F. McMorrow,¹⁰ M. Orendáč,⁶ A. Orendáčová,⁶ D. McK. Paul,⁵ R. I. Smith,² M. T. F. Telling,² and A. Wildes⁴

¹University College London, Department of Chemistry, 20 Gordon Street, London WC1H 0AJ, United Kingdom

²ISIS Facility, Rutherford Appleton Laboratory, Chilton, Didcot, Oxon, OX11 0QX, United Kingdom

³Laboratoire de Physique, Ecole Normale Supérieure, 46 Allée d'Italie, F-69364 Lyon, France

⁴Institut Laue-Langevin, 6 rue Jules Horowitz, BP 156 - 38042 Grenoble Cedex 9, France

⁵Department of Physics, University of Warwick, Coventry, CV4 7AL, United Kingdom

⁶Department of Physics, P. J. Šafárik University, 041 54 Košice, Slovakia

⁷The Royal Institution of Great Britain, 21 Albemarle Street, London W1X 4BS, United Kingdom

⁸Department of Physics, Brookhaven National Laboratory, Upton, New York 11973-5000, USA

⁹NIST Center for Neutron Research, Gaithersburg, Maryland 20899-8562, USA

¹⁰Risø National Laboratory, P.O. 49, DK-4000 Roskilde, Denmark

(Received 18 April 2003; published 16 July 2003)

Er₂Ti₂O₇ has been suggested to be a realization of the frustrated $\langle 111 \rangle$ XY pyrochlore lattice antiferromagnet, for which theory predicts fluctuation-induced symmetry breaking in a highly degenerate ground state manifold. We present a theoretical analysis of the classical model compared to neutron scattering experiments on the real material, both below and above $T_N = 1.173(2)$ K. The model correctly predicts the ordered magnetic structure, suggesting that the real system has order stabilized by zero-point quantum fluctuations that can be modeled by classical spin wave theory. However, the model fails to describe the excitations of the system, which show unusual features.

DOI: 10.1103/PhysRevB.68.020401

PACS number(s): 75.10.-b, 28.20.Cz, 75.25.+z

An important aspect of condensed matter is the separation of energy scales, such that the minimization of one set of interactions may result in the frustration of another. A paradigm is the frustrated antiferromagnet, in which the local magnetic couplings between ions are frustrated by the crystal symmetry that the ions adopt. However, a systematic study of the rare earth pyrochlore titanates $R_2\text{Ti}_2\text{O}_7$ has shown that local antiferromagnetic bond frustration is neither a necessary, nor a sufficient condition for magnetic frustration.¹⁻⁵ Rather, it arises from the interplay, in the context of the crystal symmetry, of the principal terms in the spin Hamiltonian. In the case of $R_2\text{Ti}_2\text{O}_7$, the main terms are single-ion anisotropy, exchange and dipolar coupling. Depending on the balance of these factors, one observes spin ice behavior ($R = \text{Ho}, \text{Dy}$),¹⁻³ spin liquid behavior ($R = \text{Tb}$),⁴ and dipole induced partial order ($R = \text{Gd}$).⁵

Such behavior is best classified in terms of the dominant $\langle 111 \rangle$ single-ion anisotropy that arises from the trigonal crystal electric field (CEF) at the rare earth site. For example, whereas the Heisenberg antiferromagnet has a spin liquid ground state,⁶ the $\langle 111 \rangle$ Ising (dipolar) ferromagnet has a spin ice ground state.^{1,3,7} There is thus a clear motivation to study models based on other simple anisotropies and their realization in the titanate series. In this paper we study one such model the $\langle 111 \rangle$ XY model antiferromagnet⁸ and its realization Er₂Ti₂O₇.⁹⁻¹²

We consider the Hamiltonian

$$H = -J \sum_{\langle i,j \rangle} \vec{S}_i \cdot \vec{S}_j - D \sum_i (\vec{S}_i \cdot \vec{d}_i)^2, \quad (1)$$

where the classical spins \vec{S}_i populate a face centered cubic array of corner sharing tetrahedra: the pyrochlore lattice. The spins are confined to easy XY planes by a local $d_i = \langle 111 \rangle$ anisotropy $D < 0$ and are coupled antiferromagnetically by exchange $J < 0$. This model was first studied in Ref. 8, where a discrete, but macroscopically degenerate, set of ground states was identified. At finite temperature thermal fluctuations were found to select an ordered state by the mechanism that Villain called “order by disorder”¹³ and a first order phase transition was observed in numerical simulations. The propagation vector of the ordered state was found to be $\mathbf{k} = 0, 0, 0$ (henceforth “ $k=0$ ”), but the basis vectors of the magnetic structure were not determined. We have recently discovered that the ground state degeneracy is more extensive than suggested in Ref. 8; that there exists a continuous manifold of $k=0$ ground states and that there may even be disordered states with continuous internal degrees of freedom.¹²

The possible basis states of the $k=0$ manifold were identified by group theory methods. They transform as linear combinations of the basis vectors of four irreducible representations (IR's), labeled $\Gamma_{3,5,7,9}$.¹⁴ The XY anisotropy energy is minimized only by (a) linear combinations of the two basis vectors $\psi_{1,2}$ that transform as the second order IR Γ_5 , (b) the discrete set of symmetrically equivalent basis vectors ψ_{3-5} that transform as the third order IR Γ_7 (see Fig. 1). Monte Carlo simulations confirmed that the first order transition at $T_N/J = 0.125$ selects $k=0$ order. An analysis of the distribution of bond energies suggested that immediately below T_N there remains a continuous degeneracy in the $k=0$ manifold.¹² As $T \rightarrow 0$, the spins were found to settle gradu-

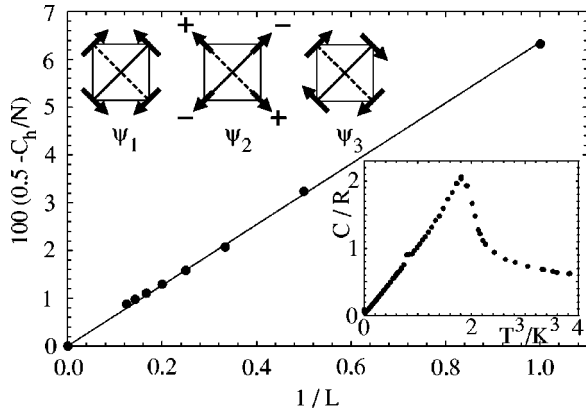


FIG. 1. Upper inset: tetrahedral basis projected down [001], from left to right: ψ_1 , ψ_2 , ψ_3 . \pm denotes how spins tilt out of the plane (they lie parallel to the opposite triangular face of the tetrahedron). Graph: size dependence of the simulated specific heat for $N=16L^3$ spins. Lower inset: experimental low temperature specific heat vs T^3 (powder sample). A turn up low at temperature, attributed to hyperfine effects (Ref. 9), is barely visible with this choice of scale.

ally into the magnetic structure defined by ψ_2 belonging to the continuously degenerate IR Γ_5 . (Note that ψ_2 is the only noncoplanar structure among ψ_{1-5} .) Both the initial selection of $k=0$ and the final selection of ψ_2 must be order by disorder processes as the ground state manifold is macroscopically degenerate.

To understand this ground state selection, we analyze the $D/J \rightarrow \infty$ model (i.e., spins confined to local XY planes). We expect that for the preferred ground state a spin wave analysis should expose the presence of zero frequency modes over an extensive region of the Brillouin zone.¹⁵ This is indeed the case: we calculate the quadratic Hamiltonian for small displacements away from a given ground state, which we symmetrize and diagonalize to find the normal mode spectrum.¹² Applying this procedure to the state ψ_2 gives eigenvalues

$$\lambda(\vec{q}) = 4J[1 \pm \cos(\vec{q} \cdot \vec{a}/2)],$$

$$\lambda(\vec{q}) = 4J\{1 \pm \cos[\vec{q} \cdot (\vec{c} - \vec{b})/2]\}, \quad (2)$$

where \vec{a} , \vec{b} , and \vec{c} , are the basis vectors of the primitive rhombohedral unit cell. Hence, there are branches with $\lambda(\vec{q})=0$ over planes in the Brillouin zone, for which $\vec{q} \cdot \vec{a} = 0$ and $\vec{q} \cdot (\vec{c} - \vec{b}) = 0$. The same procedure when applied to other selected ground states yields a microscopic number of zero modes at specific points in the zone. This difference gives the mechanism for the order by disorder selection of ψ_2 . In this approximation the amplitude of the soft modes diverges, giving a dominant contribution to the entropy.¹⁵ Evidence of the soft modes exists in the specific heat, as each contributes less than $\frac{1}{2}k_B$. As there are $O(L^2)$ modes, the quantity $\frac{1}{2} - C_h/Nk_B$ should scale as $1/L$ at low temperature, as confirmed in Fig. 1. We note that the entropy contribution to the free energy from the soft modes scales as $N^{2/3}$ and so is not extensive. While this could mean that the ordering within the $k=0$ manifold occurs at a temperature-dependent

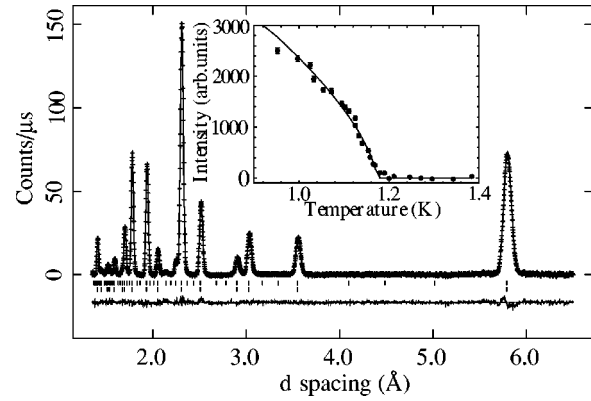


FIG. 2. Main picture: powder neutron profile refinement (POLARIS, 50 mK, $R_{wp}=1.23\%$, about a third of the intensity is magnetic). The lower line is observed minus calculated intensity. Inset: single crystal Bragg intensity [PRISMA, (2,2,0) reflection] and fit to a power law (see text).

system size that goes to zero in the thermodynamic limit, no such effect was detected in the system sizes we have studied.

Disordered states are occasionally formed in the simulations, by the rotation of columns of spins with infinite length out of an ordered state. This suggests that, starting from the ψ_2 state, one can introduce $O(L^2)$ independent column defects, all perpendicular to a given plane. Our calculation, giving $O(L^2)$ soft modes is compatible with this description and is analogous to the case of the Heisenberg kagomé antiferromagnet.¹⁵ For the latter, fluctuations out of a coplanar spin configuration can be described equivalently in terms of soft propagating modes and localized zero energy excitations.

The material $\text{Er}_2\text{Ti}_2\text{O}_7$, which orders magnetically at ~ 1.2 K,⁹ has been suggested to approximate the $\langle 111 \rangle XY$ antiferromagnet.^{10,11} To test this we have determined its magnetic structure by powder neutron diffraction using the POLARIS diffractometer (ISIS). The magnetic reflections observed below $T_N \approx 1.2$ K index with a propagation vector of $k=0$. As the transition is continuous (see below), the system is expected to order under only one of the nonzero IR's of the Er site representations: $\Gamma_{3,5,7,9}$, as defined above. Refinement of the magnetic structure¹⁶ showed that only the two basis vectors ψ_1 , ψ_2 of Γ_5 were consistent with the magnetic intensity (see Figs. 1, 2). Single crystal diffraction data collected on the instruments E2 (HMI, Berlin) and PRISMA (ISIS), allowed us to distinguish between the two structures. The measurements were performed on a (~ 8 mm³) crystal at temperatures down to 0.13 K. In order to suppress the formation of multidomains due to the cubic symmetry, a magnetic field was applied along the $[1 \bar{1} 0]$ direction. Below T_N , we found that a field of 0.5 T caused the (2,2,0) magnetic Bragg peak to increase from 260 counts to 500 counts, while the other peaks remained approximately unchanged. This increase in the (2,2,0) by a factor of 1.9 ± 0.2 is consistent with the formation of a monodomain of the ψ_2 ground state. We can conclude that the zero field ordering pattern is also described by ψ_2 , in agreement with the theory.

The ordered moment at 50 mK (where ordering is essentially complete) is $3.01 \pm 0.05 \mu_B$ per atom. A CEF analysis,¹⁷ following Ref. 18, predicts a single-ion Kramers doublet ground state with the wave function $-0.5428 |-\frac{1}{2}\rangle - 0.2384 |-\frac{5}{2}\rangle + 0.5628 |\frac{1}{2}\rangle + 0.3876 |\frac{7}{2}\rangle - 0.426 |\frac{13}{2}\rangle$. This corresponds to moments of $3.8 \mu_B$ and $0.12 \mu_B$ perpendicular and parallel to $\langle 111 \rangle$. In an antiferromagnet, zero-point quantum fluctuations significantly reduce the ordered moment from the single-ion value. The observed moment of $3.01 \mu_B$, thus, agrees well with quasi-classical ordering of local XY -like moments with a magnitude fixed by the CEF.

The dominant perturbation to the model Hamiltonian in Er₂Ti₂O₇ are dipole-dipole interactions¹¹ and one might speculate that these are the true cause for the ψ_2 ordering. In the Heisenberg pyrochlore antiferromagnet, provided the ratio of dipolar energy to near neighbor exchange is less than a critical value, $J_{dd}/J_{nn} < 5.7$, the ground state is an energetically selected $k=0$ state: the ψ_3 basis (Fig. 1).^{19,20} As this state is also a ground state for the $\langle 111 \rangle XY$ model, it is clear that in the present case it will be stabilized by dipolar interactions. We expect Er₂Ti₂O₇ to have $J_{dd}/J_{nn} \ll 5.7$, and thus ψ_3 order, contrary to observation. With a moment of $3 \mu_B$ the near neighbor dipolar interaction has a magnitude -0.32 K per spin for ψ_3 and $+0.06$ K per spin for $\psi_{1,2}$. It is therefore a substantial fraction of T_N . However, zero point quantum fluctuations also stabilize the ground state of an antiferromagnet and will favor the softer ψ_2 state.²¹

We are therefore drawn to the conclusion that the most likely cause of the observed ψ_2 order in Er₂Ti₂O₇ is its stabilization by zero-point quantum fluctuations, the effect of which is captured by our classical spin wave calculation. However, the close agreement of experiment and theory does not extend to the excitations of the system, as we now discuss.

In our model, the density of classical spin wave states, $g(\lambda)$ is a constant, a result that is incompatible with the experimental specific heat, which shows a T^3 dependence up to ~ 1 K (inset, Fig. 1). Furthermore, in contradiction with theory,⁸ the ordering transition was found to be continuous within experimental precision. The evolution of the magnetic Bragg peaks near the critical temperature $T_N = 1.173(2)$ K obeys a standard power law with the critical exponent $\beta = 0.33(2)$, characteristic of the 3D- XY model (inset, Fig. 2).²² This observation of a conventional β provides a counter example to the idea²³ that pyrochlore antiferromagnets represent a *new* universality class, analogous to Kawamura's chiral universality class for triangular lattice antiferromagnets.²⁴

To investigate the excitations further, the dynamics of Er₂Ti₂O₇ have been investigated by inelastic neutron scattering. Measurements were carried out on the spectrometers PRISMA (ISIS), RITA (Risø National Laboratory), and IN14 (ILL). For a powder sample, excitons²⁵ were found at 6.3 and 7.3 meV [Fig. 3(a)]. Their dispersion can be fitted to $E(Q) = \sqrt{\Delta^2 - 2a^2 J(Q)\Delta}$ with $\Delta = 6.38(1)$ meV, $a\sqrt{J(0)} = 0.35(1)$ meV^{1/2} for the lower level and $\Delta = 7.39(1)$ meV, $a\sqrt{J(0)} = 0.21(1)$ meV^{1/2} for the upper

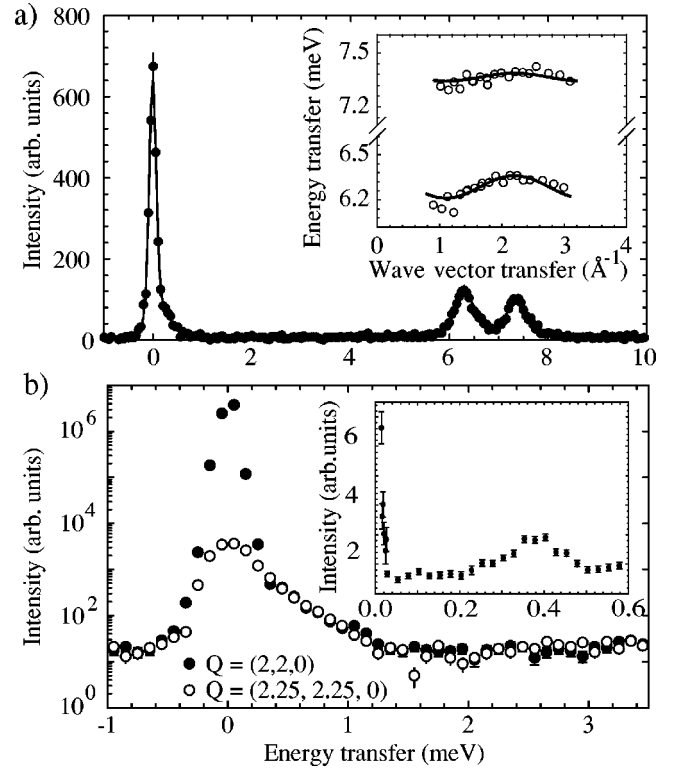


FIG. 3. (a) Powder inelastic spectrum (PRISMA, 1.8 K, $|\mathbf{Q}| = 1.1 \text{ \AA}^{-1}$). Inset: wave vector dependence of the excitation energies fitted to a cosine variation. (b) Single crystal inelastic scattering (IN14, 100 mK, the strong elastic signal is Bragg scattering). Inset: Powder inelastic scattering (IRIS, 50 mK), integrated over 15 spectra from $|\mathbf{Q}| = 0.41 \text{ \AA}^{-1}$.

level. Here, $J(Q)$ is the Fourier transformed exchange and a is related to the matrix elements that connect the ground and excited states.^{26,27} The values of Δ compare with the CEF predictions of 6.4 and 8.8 meV,¹⁷ while $J(0)/k_B$ is implied to be at least 1.5 K. Dispersed excitons are also observed in Tb₂Ti₂O₇.⁴

In the lower energy scale, data from an image-furnace grown single crystal ($\sim 250 \text{ mm}^3$) reveal a shoulder of scattering on the elastic line extending out to ~ 1.5 meV [Fig. 3(b)]. This shoulder, which does not appear to obey a strong wave vector dependence [Fig. 3(b)], gradually weakens upon heating above T_N . High resolution scans on PRISMA ($T = 0.08$ K) and on a powder sample on the IRIS spectrometer at ISIS [inset, Fig. 3(b)] resolved the shoulder into a peak at 0.4 meV, with a width outside the instrumental resolution.

One possible explanation, that this peak is a very low lying CEF level, as invoked by Blöte *et al.*⁹ to explain the anomalously large Curie-Weiss temperature $\theta = -22$ K is not consistent with the predicted CEF scheme.¹⁷ A more natural explanation is that it is a weakly dispersed optical magnon mode. Evidence for a gapped magnon spectrum is provided by the IRIS data [inset, Fig. 3(b)], which is at the level of background between 0.03 meV (~ 0.3 K) and 0.2 meV (~ 2 K), indicating an absence of magnons in this range. However, there is a problem with this interpretation:

the T^3 specific heat (inset, Fig. 1) requires a density of un-gapped excited states that increases quadratically with energy up to at least ~ 1 K. One possible way out of this conundrum is to invoke the existence of a hidden branch of excitations that do not couple directly to neutrons. It is interesting to note that frustrated, quasi-two-dimensional $\text{SrCr}_x\text{Ga}_{12-x}\text{O}_{19}$ and $(\text{H}_3\text{O})\text{Fe}_3(\text{SO}_4)_2(\text{OH})_6$ have T^2 specific heats despite the absence of conventional magnons.^{28,29}

A final point of interest is that the other erbium pyrochlores $\text{Er}_2\text{GaSbO}_7$ and $\text{Er}_2\text{Sn}_2\text{O}_7$ apparently do not order down to 50 mK.^{9,30} It is possible that in this family there is a kind of quantum critical point where as a function of the interionic couplings, quasiclassical order gives way to the quantum fluctuations of the single ion doublets. Similar

effects might also be relevant for $\text{Tb}_2\text{Ti}_2\text{O}_7$,^{4,31,32} $\text{Yb}_2\text{Ti}_2\text{O}_7$,³³ and spinels such as ZnCr_2O_4 .³⁴

In conclusion, the simplest theoretical model of $\text{Er}_2\text{Ti}_2\text{O}_7$, in which the single-ion moment is fixed by the CEF, the dipolar interaction is ignored and the exchange is treated quasi-classically, yields the correct ground state properties and furnishes strong evidence of quantum order by disorder. However, it fails to describe the unusual excitation spectrum of the system and does not encompass the behavior of $\text{Er}_2\text{GaSb}_2\text{O}_7$ and $\text{Er}_2\text{Sn}_2\text{O}_7$. A detailed understanding of $\text{Er}_2\text{Ti}_2\text{O}_7$ thus leaves an intriguing challenge for future research.

It is a pleasure to thank H.-B. Braun, B. Canals, M. J. P. Gingras, J. A. Hodges, and C. Lacroix for useful discussions and R. Down for technical assistance.

*Author for correspondence: s.t.bramwell@ucl.ac.uk

¹M. J. Harris *et al.*, Phys. Rev. Lett. **79**, 2554 (1997).

²A. P. Ramirez *et al.*, Nature (London) **399**, 333 (1999).

³S. T. Bramwell *et al.*, Phys. Rev. Lett. **87**, 047205 (2001).

⁴J. S. Gardner *et al.*, Phys. Rev. Lett. **82**, 1012 (1999).

⁵J. D. M. Champion *et al.*, Phys. Rev. B **64**, 140407(R) (2001).

⁶R. Moessner and J. T. Chalker, Phys. Rev. Lett. **80**, 2929 (1998); B. Canals and C. Lacroix, Phys. Rev. B **61**, 1149 (2000).

⁷B. C. den Hertog and M. J. P. Gingras, Phys. Rev. Lett. **84**, 3430 (2000).

⁸S. T. Bramwell, M. J. P. Gingras, and J. N. Reimers, J. Appl. Phys. **75**, 5523 (1994).

⁹H. W. J. Blöte *et al.*, Physica (Amsterdam) **43**, 549 (1969).

¹⁰M. J. Harris *et al.*, J. Magn. Magn. Mater. **177**, 757 (1998).

¹¹R. Siddharthan *et al.*, Phys. Rev. Lett. **83**, 1854 (1999).

¹²J. D. M. Champion, Ph.D. Thesis, Univ. London, 2001.

¹³J. Villain, J. Phys. (France) **41**, 1263 (1980).

¹⁴These are a subset of the nine IRs, $\Gamma_{1 \dots 9}$, that describe all possible $k=0$ spin configurations in the crystallographic space group $Fd\bar{3}m$. The numbering follows the scheme defined in O. V. Kovalev, *Representations of the Crystallographic Space Groups*, ed. 2 (Gordon and Breach Science Publishers, Switzerland, 1993).

¹⁵J. T. Chalker, P. C. W. Holdsworth, and E. F. Shender, Phys. Rev. Lett. **68**, 855 (1992).

¹⁶Using the SARA*h* program, A. S. Wills, Physica B **276–278**, 680 (2000), in combination with GSAS, A.C. Larsen and R.B. von Dreele, *General Structure Analysis System* (Los Alamos National Laboratory, Los Alamos, 1994).

¹⁷We thank M. Rams and J. A. Hodges for provision of details of the CEF and for a useful discussion concerning the single-ion moment.

¹⁸S. Rosenkranz *et al.*, J. Appl. Phys. **87**, 5914 (2000).

¹⁹S. E. Palmer and J. T. Chalker, Phys. Rev. B **62**, 488 (2000).

²⁰If $J_{dd}/J_{nn} > 5.7$, a state with $k \neq 0$ is favored (Ref. 19).

²¹Another possible perturbation to the simple model, further neighbor exchange interactions, can be shown by symmetry not to break the degeneracy of the $k=0$ ground state [J. D. M. Champion (unpublished)].

²²The data suggest a slight systematic increase in β as T_N is approached, with $0.31 < \beta < 0.36$.

²³J. N. Reimers *et al.*, Phys. Rev. B **45**, 7295 (1992).

²⁴H. Kawamura, J. Phys. Soc. Jpn. **58**, 584 (1989).

²⁵M. T. Hutchings in *Electronic States of Inorganic Compounds: New Experimental Techniques*, edited by P. Day, Nato ASI Series, Vol. 20 (Reidel, Dordrecht, 1974).

²⁶B. Grover, Phys. Rev. A **140**, A1944 (1965).

²⁷Modeling of the dispersion would require a full and very accurate knowledge of the CEF wave functions (Ref. 25).

²⁸A.P. Ramirez, G.P. Espinosa, and A.S. Cooper, Phys. Rev. Lett. **64**, 2070 (1990).

²⁹A. S. Wills *et al.*, Europhys. Lett. **42**, 325 (1998).

³⁰K. Matsuhira *et al.*, J. Phys. Soc. Jpn. **71**, 1576 (2002).

³¹S.-H. Lee *et al.*, Phys. Rev. B **56**, 8091 (1997).

³²I. Mirebeau *et al.*, Nature (London) **420**, 54 (2002).

³³J. Hodges *et al.*, Phys. Rev. Lett. **88**, 077204 (2002).

³⁴S.-H. Lee *et al.*, Phys. Rev. Lett. **84**, 3718 (2000).